Pergamon

PII: S0277-5387(96)00482-2

Polyhedron Vol. 16, No. 10, pp. 1605–1614, 1997

0277-5387/97 $17.00+0.00

A family of mixed ligand complexes of Ru^{II}-L [L = N-aryl-pyridine-2-aldimine], their reactions, isolation and characterization. X-ray crystal structure of $[Ru(pic)(L^1)_2][ClO_4] \cdot CH_2Cl_2$ [pic = 2-picolinate ion]

Kedar Nath Mitra,[a] Subrata Choudhury,[a] Sreebrata Goswami[a]* and Shie-Ming Peng[b]

[a]Department of Inorganic Chemistry, Indian Association for the Cultivation of Science, Calcutta 700 032, India

[b]Department of Chemistry, National Taiwan University, Taipei, Taiwan, R. O. C.

(Received 6 August 1996; accepted 25 September 1996)

Abstract—Synthesis of the tris-chelated complexes $[Ru(L)_n(L^3)_{3-n}]^{2+}$ (L = *N*-aryl-pyridine-2-aldimine, L^3 = 2-(*m*-tolylazo)pyridine) based on silver(I) assisted *trans*-metallation is described. The complexes, $[Ru(L)_3]^{2+}$ and $[Ru(L)(L^3)_2]^{2+}$ afford $[Ru(pic)(L)_2]^+$ and $[Ru(pic)(L^3)_2]^+$ (pic = 2-picolinate ion) respectively, on hydrolysis and subsequent oxidation. When $RuCl_2(L)_2$ was reacted with two moles of $[Ag(L^3)_2]^+$, a pink complex of composition $[Ru(L)(L^3)(L^4)]^+$ [L^4 = *N*-aryl-2-picolinamide] was isolated along with the expected brown complex, $[Ru(L^3)(L)_2]^{2+}$. Initial oxidation of the metal ion favours L → L^4 conversion. The complexes have been characterized using spectroscopy and X-ray crystallography. The X-ray structure of $[Ru(pic)(L^1)_2]ClO_4 \cdot CH_2Cl_2$ is reported. The metal oxidation as well as ligand reductions for the complexes have been studied voltammetrically in acetonitrile using platinum as the working electrode. It has been observed that the oxidation of the transformed complexes, *viz.* $[Ru(pic)(L)_2]^+$, $[Ru(pic)(L^3)_2]^+$ and $[Ru(L)(L^3)(L^4)]^+$ occur at lower potentials as compared to their parent $[Ru(L)_n(L^3)_{3-n}]^{2+}$ complexes. All the complexes show metal-to-ligand charge transfer transitions in the visible range and absorption energies linearly correlate with the differences between the metal oxidation and the first ligand reduction potentials.

Keywords: ruthenium; Schiff-base; structure; ligand transformations; redox and redox-spectra correlation.

This work stems from our interest in the ruthenium-diimine complexes. This class of compounds is important [1] due to their rich redox and optical properties. In this respect, we have been working [2–4] on the synthesis and reactivities of ruthenium complexes of *N*-aryl-pyridine-2-aldimine (**1**, L). These complexes [2–6] are intensely coloured, undergo multiple electron transfer and most importantly, they show interesting patterns of chemical as well as photochemical reactivities.

Herein we report the synthesis and characterization of the tris-chelated ruthenium complexes involving L and L^3. These may be conveniently synthesized starting from ruthenium bis-chelated dichlorides by the use of silver(I) assisted *trans* metallation reaction route. The study of reactions of ruthenated L in the above complexes forms an important part of the present work. Interestingly, different products were obtained from apparently similar types of reactions. All the relevant species have been fully characterized. The reason for transformation selectivity of L is discussed on the basis of the present findings and other results [3,4] from this laboratory and elsewhere.

*Author to whom correspondence should be addressed.

RESULTS AND DISCUSSION

A. *The synthetic reactions*

In the process of synthesizing [2, 7–9] mixed ligand tris-chelated ruthenium complexes of L (**1**) and 2-(*m*-tolylazo)pyridine (L^3, **2**) some unusual products were

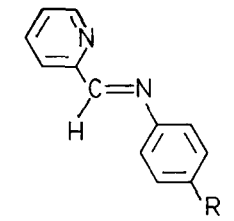

R = H : L^1
R = Me : L^2

1, L

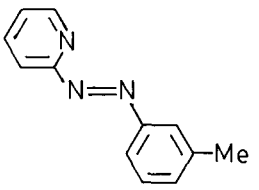

L^3

2

obtained along with the expected products, which are elaborated below. The general reaction which has been studied may be represented as follows:

$$cis\text{-}RuCl_2L'_2 + 2AgL''_2 \xrightarrow[\substack{L',L''\\ L' = L,L^3\\ L'' = L,L^3}]{EtOH} RuL_2L'' + 2AgCl + 3L'$$

(a) (i) *Reaction of cis-*$RuCl_2(L)_2$ *and two moles of* $Ag(L)_2^+$

The bluish green *cis* isomer [3] of $RuCl_2(L)_2$ was reacted with two moles of silver complex [10], $Ag(L)_2^+$, in 1 : 1 aqueous ethanol. In addition to the expected [2] brown tris-chelate, $Ru(L)_3^{2+}$ (**3**), a pink compound was also formed. Interestingly, an aqueous ethanolic solution of pure $Ru(L)_3^{2+}$ in the presence of dilute aqueous $AgNO_3$ quantitatively produced the pink compound. The pink product was purified on a silica gel column eluting with 1 : 5 CH_3CN-CH_2Cl_2 mixture. The brown product was obtained from the column using a more polar solvent (2 : 3 CH_3CN-CH_2Cl_2 mixture) as an eluent.

(ii) *Characterization*

The brown compound was identified as the known [2] $[Ru(L)_3](ClO_4)_2 \cdot H_2O$ (**3**) which we do not discuss any further. The pink compound which analyzed as $[Ru(pic)(L)_2]ClO_4 \cdot CH_2Cl_2$ (**4**) (pic = 2-picolinate anion) is diamagnetic and a 1 : 1 electrolyte in CH_3CN. The IR spectrum showed all the characteristic features [2, 3] of coordinated L and ionic ClO_4^-. Interestingly, it also displayed a moderately strong band at 1650 cm^{-1} indicating the presence [11] of a carboxylic function. Selected characterization data are collected in Table 1.

Fortunately, single crystals of **4** (L = L^1) could be grown as solvates: **4**·CH_2Cl_2 and its structure was successfully solved crystallographically. Molecular views of the complex excluding the solvent of crystallization and the counter anion, ClO_4^- are shown in Fig. 1. Selected bond distances and bond angles are collected in Table 2. The structure solution of **4** unequivocally confirms the composition of **4** as $Ru(pic)(L^1)_2^+$. The geometry of the $Ru(L^1)_2$ fragment in **4** is *trans*, *cis* (*trans* with respect to two N^1(py) and *cis* with in the N^2 (imine) pair). The carboxylic function lies *trans* to one of the two imine nitrogens. In this manner the three pyridine nitrogens are positioned meridionally. We note here that the parent complex **3** exists [2] in the meridional geometry. Therefore, the transformation **3** → **4** is stereoretentive.

In the above structure, Ru—N(5) length agrees [12] well with the Ru—N lengths in $Ru(pic)_2(PPh_3)_2$. Interestingly, the four Ru—N lengths in the $Ru(L^1)_2$ fragment of **4** are not equal. The Ru—N(4) length is notably shorter than other three Ru—N lengths. This must be due to stronger $d\pi$–$p\pi$ interactions [13] between Ru^{II} and π^* of the imine function containing N(4), which lies *trans* to the strong σ-donor carboxylic acid function. Moreover, the average Ru—N (imine) length in **4** is shorter [4] by *ca* 0.03 Å compared to that in *trans*-$Ru^{III}(L^1)(L^4)Cl_2$ (L^4 = N-phenyl-2-picolinamide). This may be attributed to the superior back-bonding in ruthenium(II) complexes.

Finally, it may be noted that the reaction of hydrated $RuCl_3$ and $Ag(L)_2^+$ in 1 : 3 mole ratio also resulted in the formation of a mixture of **3** and **4**. The yield of **4** increases with the increase of the duration of the reaction.

The reactions, described above, are schematically presented in Scheme I.

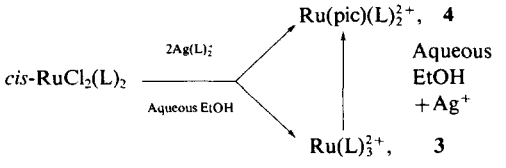

Scheme I

Table 1. Characterization data

Compound	IR(cm^{-1})[a] $\nu_{C=O}$ (carboxylic acid)	$\nu_{C=O}$ (amide)	$\nu_{C=N}$	Λ_m[b] (ohm $^{-1}cm^2mol^{-1}$)	δMe[c] (ppm)
$[Ru(L^1)_3](ClO_4)_2 \cdot H_2O$			1610	210	
$[Ru(pic)(L^1)_2]ClO_4 \cdot CH_2Cl_2$	1650		1610	115	
$[Ru(L^2)_3](ClO_4)_2 \cdot H_2O$			1610	219	2.18, 2.08
$[Ru(pic)(L^2)_2]ClO_4 \cdot CH_2Cl_2$	1650		1610	120	2.15, 2.05
$[Ru(L^2)(L^3)_2](ClO_4)_2 \cdot H_2O$			1600, 1610	221	2.12, 2.21
$[Ru(pic)(L^3)_2]ClO_4 \cdot CH_2Cl_2$	1660		1610	126	2.21, 2.13
$[Ru(L^3)(L^2)_2](ClO_4)_2 \cdot H_2O$			1595, 1610	205	2.21, 2.16
$[Ru(L^2)(L^3)(L^4)]ClO_4 \cdot CH_2Cl_2$		1620	1595	105	2.30, 2.25, 2.16

[a] In KBr dist.
[b] In MeCN at 298 K with a solute concentration of *ca* 10^{-3} mol.
[c] In $CDCl_3$ using $Si(Me)_4$ as the internal standard.

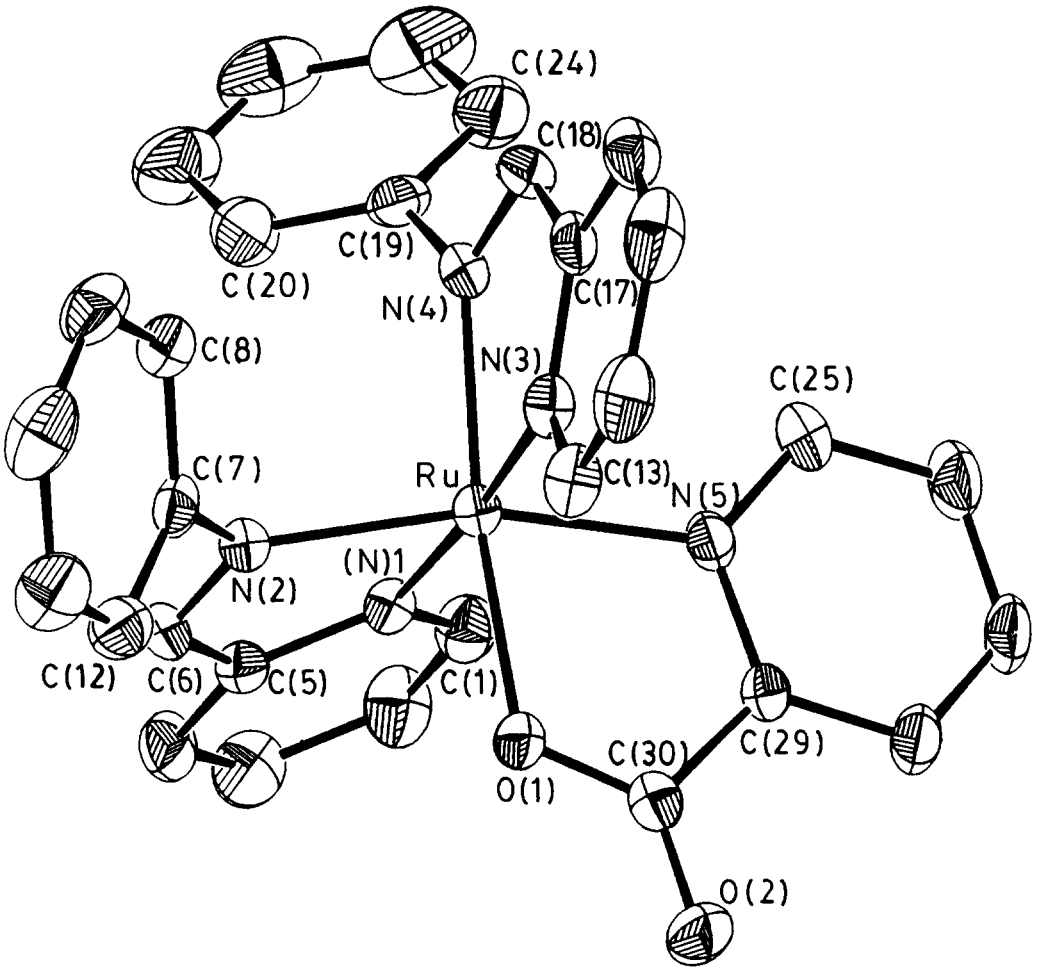

Fig. 1. ORTEP plot and atom labelling scheme for $Ru(pic)(L^1)_2$ in $[Ru(pic)(L^1)_2]ClO_4 \cdot CH_2Cl_2$.

Table 2. Selected bond distances (Å) and angles (°) and their estimated standard deviations for $[Ru(pic)(L^1)_2]ClO_4 \cdot CH_2Cl_2$

Ru—N(1)	2.046(5)	N(2)—C(6)	1.301(8)
Ru—N(2)	2.045(5)	N(4)—C(18)	1.316(8)
Ru—N(3)	2.048(5)	O(1)—C(30)	1.285(8)
Ru—N(4)	2.022(5)	O(2)—C(30)	1.225(8)
Ru—N(5)	2.079(5)	N(2)—C(7)	1.435(8)
Ru—O(1)	2.073(4)	N(4)—C(19)	1.435(8)
N(1)—Ru—N(2)	78.34(21)	N(2)—Ru—O(1)	87.29(18)
N(1)—Ru—N(3)	176.18(20)	N(3)—Ru—N(4)	78.91(21)
N(1)—Ru—N(4)	99.63(20)	N(3)—Ru—N(5)	90.37(20)
N(1)—Ru—N(5)	93.29(20)	N(3)—Ru—O(1)	93.83(19)
N(1)—Ru—O(1)	87.92(19)	N(4)—Ru—N(5)	95.60(20)
N(1)—Ru—N(3)	98.33(21)	N(4)—Ru—O(1)	171.27(19)
N(2)—Ru—N(4)	98.48(20)	N(5)—Ru—O(1)	79.47(18)
N(2)—Ru—N(5)	164.63(20)		

(b)(i) *Reaction of cis-*$RuCl_2(L^3)_2$ *and two moles of* $Ag(L)_2^+$

Similar to the prior reaction, this reaction also resulted in the formation of two major products, one of which is violet and the other one is brown in colour. The compounds were purified on a silica gel column by eluting with solvent mixtures of different polarities. The violet compound may be generated by boiling the brown product in aqueous ethanol in the presence of dilute $AgNO_3$ solution. Interestingly, the reaction [11] of *cis*-$Ru(OH_2)_2(L^3)_2^{2+}$ with PicH in ethanol instantaneously produces the violet product in a high yield.

(ii) *Characterization*

The first moving violet band was eluted with 5:2 CH_2Cl_2-CH_3CN mixture and it analyzed as $[Ru(pic)(L^3)_2]ClO_4 \cdot CH_2Cl_2$ (**5**). The brown product, which was eluted with 1:1 CH_2Cl_2–CH_3CN mixture, analyzed as $[Ru(L^2)(L^3)_2](ClO_4)_2 \cdot H_2O$, (**6**). The compound **5** is a 1:1 electrolyte whereas the compound **6** is 1:2 electrolyte in CH_3CN. The compound **5** displayed a moderately strong absorption at 1660 cm^{-1} in the IR spectrum. This band is conspicuously absent in the IR spectrum of **6**. Evidently, the 1660 cm^{-1} absorption indicates the presence [11] of a carboxylic function in **5** (Table 1).

The ^1H NMR spectra of the compounds **5** and **6** were examined. In this case we have used only methyl substituted ligand, L^2 to take advantage of monitoring the methyl resonances in the less crowded region of the ^1H NMR spectrum. The aromatic region of both the spectra are complex due to serious overlapping. Therefore, we concentrated only on the methyl resonances (Table 1). The compound **5** displayed two equally intense resonances at 2.15 and 2.05 δ. The intensities of two resonances correspond to six protons. The compound **6** also displayed two methyl resonances at 2.21 and 2.12 δ, but the ratio of signal intensities is 1:2. Moreover, the total area covered by the two methyl signals of **6** corresponded to nine protons. Therefore, it may be concluded that the two equally intense methyl resonances in **5** is due to the presence of two L^3 ligands. In the spectrum of **6** there are three methyl resonances, two of which are overlapping which are attributed [14] to methyl groups of L^3, and the second signal is due [2] to the *p*-tolyl group of L^2. The spectral data, presented above, clearly demonstrate that the hydrolytic oxidative cleavage of an imine function occurs in the formation of **5**.

Thus, the reaction is similar to the reaction which is described in Section (a).

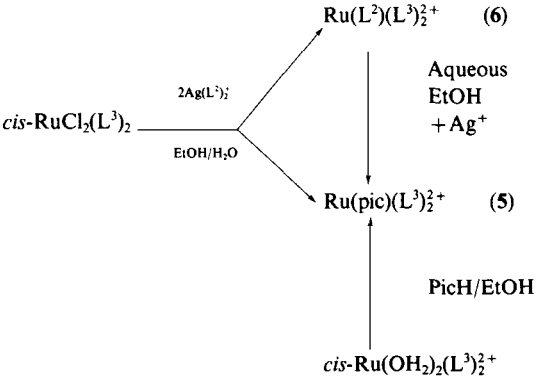

Scheme II

(c) (i) *Reaction of cis-*$RuCl_2(L^2)_2$ *and two moles of* $Ag(L^3)_2^+$

In this reaction bluish green *cis* isomer of $RuCl_2(L^2)_2$ was reacted with two moles [15] of $Ag(L^3)_2^+$ in aqueous ethanol. This reaction also yielded two major products. One of the two products is pink whereas the other one is brown. Unlike the two previously described reactions, the brown product is quite stable in boiling aqueous ethanol. Both the

products were purified by using the column chromatography technique.

(ii) *Characterization*

The pink product was eluted with 1:9 CH_3CN-CH_2Cl_2 solvent mixture and analyzed as $[Ru(L^2)(L^3)(L^4)](ClO_4)_2 \cdot 0.5CH_2Cl_2$ (L^4 = N-*p*-tolyl-2-picolinamide), (**7**). The brown product was then eluted with 1:1 CH_3CN-CH_2Cl_2 mixture. Based on the elemental analyzes the composition was ascertained as $[Ru(L^3)(L^2)_2](ClO_4)_2 \cdot H_2O$ (**8**). The characterization of **7** and **8** were unambiguously made based on their physical data.

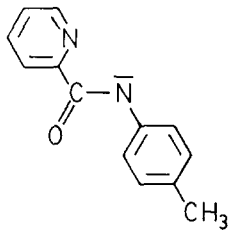

L^4

The compounds **7** and **8** are 1:1 and 1:2 electrolytic, respectively, in acetonitrile. Unlike monopicolinates, the compound **7** did not show any characteristic absorption of carboxylic function. Instead, a moderately strong band at 1620 cm^{-1} in the IR spectrum of **7** confirms the presence [4, 13] of an amide function. Fortunately, this compound (**7**) displayed highly resolved ^1H NMR spectrum (Fig. 2) which was conveniently used for its characterization. The spectrum consists of well separated, equally intense three methyl resonances between 2.1–2.3 δ. This clearly reveals the presence of three tolyl groups in **7**. Moreover, there are four doublets of 2H intensities in the range 7.0 to 5.5 δ. Such doublets of two proton intensities can only arise from *p*-tolyl groups in this compound. The rest of the spectrum is complex due to overlapping peaks. The ^1H NMR spectrum of **8**, as expected, consists of two methyl resonances, one of which is double the intensity of the other. The spectral data collectively taken with the analytical data do conform to the proposed composition of the above compounds.

The reaction, described above, may then be summarized below in Scheme III.

We note that a tris-chelated compound with three different bidentate ligands as in **7** is extremely rare [16].

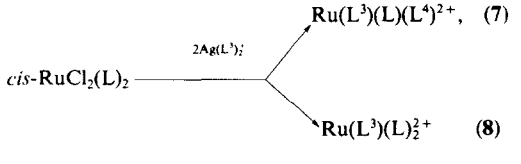

Scheme III

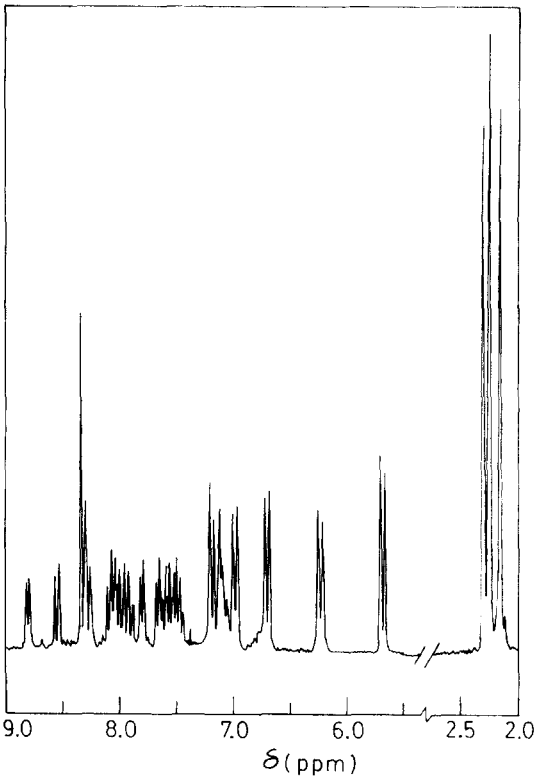

Fig. 2. ^1H NMR spectrum of $[Ru(L^2)(L^3)(L^4)]ClO_4 \cdot CH_2Cl_2$ in $CDCl_3$.

B. *The origin of transformations*

The reactions described above may be broadly classified in two categories: type (i) L → pic (reactions (a) and (b)); type (ii) L → L^4 (reaction (c)). We first consider the reaction (b) of type (i). In this reaction the starting ruthenium compound does not contain L. Therefore, the formation of $[Ru(pic)(L^3)_2]^+$ could, in principle, occur in two ways. Once the coordinated chlorides are precipitated as insoluble AgCl, the solution mixture then contains bis-solvento complex, $RuS_2(L^3)_2^{2+}$ (S = solvent) and four moles of free L. Coordination of L to $Ru(L^3)_2^{2+}$ moiety would produce $Ru(L)(L^3)_2^{2+}$ (**6**). Furthermore, hydrolysis [17] of an imine function in a hydroxylic solvent is a common phenomenon. Thus, hydrolysis of free L followed by oxidation of the aldehyde function would produce PicH in solution which may then react with the labile bis-solvento species to form the monopicolinate, **5**. The second possibility is the same transformation of L occurring after coordination to $Ru(L^3)_2^{2+}$ moiety. We note here that **6** can be easily transformed to **5** and the electrophilicity of L increases upon coordination, which is primary for the hydrolysis of an imine function. Out of the above two possibilities, we therefore propose that L → pic transformation presumably occurs *via* coordination of L. This proposal also applies to the reaction (a).

Table 3. Cyclic voltammetric data[a]

Compound	Metal-centred oxidation $E_{1/2}$(V)[E_p(mV)]	Ligand-based reductions $-E_{1/2}$(V)[ΔE_p(mV)]
$[Ru(L^1)_3](ClO_4)_2 \cdot H_2O$	1.43(75)	0.93(90), 1.16(100), 1.49(110)
$[Ru(pic)(L^1)_2]ClO_4 \cdot CH_2Cl_2$	1.00(75)	1.15(100), 1.48(90)
$[Ru(L^2)_3](ClO_4)_2 \cdot H_2O$	1.44(70)	0.90(90), 1.19(110), 1.52(110)
$[Ru(pic)(L^2)_2]ClO_4 \cdot CH_2Cl_2$	1.00(80)	1.16(100), 1.48(100)
$[Ru(L^2)(L^3)_2](ClO_4)_2 \cdot H_2O$	2.00[b]	0.15(90), 0.65(100), 1.56(170)
$[Ru(pic)(L^3)_2]ClO_4 \cdot CH_2Cl_2$	1.56(70)	0.28(100), 0.85(100), 1.71(180)
$[Ru(L^3)(L^2)_2](ClO_4)_2 \cdot H_2O$	1.81[b]	0.40(90), 1.05(100), 1.57(120)
$[Ru(L^2)(L^3)(L^4)](ClO_4)_2 \cdot CH_2Cl_2$	0.98(70)	0.92(100), 1.27(100)

[a] Cyclic voltammetric experiments were carried out in MeCN at 298 K using 0.1 mol NBu_4ClO_4 as supporting electrolyte and platinum as working electrode. The reported data correspond to scan rate $v = 50$ mV s^{-1}.

[b] Irreversible response, the potential corresponds to E_{pa}.

The other type of transformation, $L \rightarrow L^4$ (type (ii)) must occur with the coordinated L since both L are already coordinated in the starting material. This type of transformation of an imine function has been exemplified [4,13] very recently, in two other ruthenium systems. One such example is the oxidative transformation of *trans*-$Ru^{II}Cl_2(L)_2$ to *trans*-$Ru^{III}Cl_2(L)(L^4)$. It has been shown that initial oxidation of the metal ion followed by partial hydrolysis of coordinated L^1 and subsequent oxidation of the hydrolyzed L are the steps involved in the above transformation. At this stage, comparison of oxidation power of different reactants of reaction (c) is necessary for further discussion. We note that L^3 is a very strong [14] π-acceptor. Consequently, $Ag(L^3)_2^+$ should be a strong oxidant. Furthermore, the oxidation of *cis*-$RuCl_2(L)_2$ may be easily achieved [3] ($E_{1/2}$: 0.32 V). In the reaction (c), initial oxidation of $RuCl_2(L)_2$ by $Ag(L^3)_2^+$ is, therefore, the most plausible one. The oxidation of the metal ion then leads to an identical situation where coordinated $L \rightarrow L^4$ transformation was shown [4] to occur by the oxidation of the metal centre. In contrast to the previously reported examples [4,13], initial oxidation of the metal ion in reaction (c) is not reflected in the oxidation state of the same in the final product. In the present case (**7**) beside being coordinated to L^4, ruthenium is also bound to a very strong π-acceptor, L^3 and a moderate acceptor L. In the environment of L, L^3 and L^4, ruthenium is preferably stabilized in the bivalent state ($E_{1/2}$: Ru^{III}/Ru^{II} 1.0 V *vide infra*).

It may, therefore, be concluded, from the foregoing discussion, that hydrolysis followed by oxidation of coordinated L results in the formation of pic, whereas oxidation of the compound followed by hydrolysis would preferentially transform L to L^4.

C. *Electrochemical properties and redox-spectra correlation*

Electrochemical properties of the compounds **3**–**8** were studied cyclic voltammetrically in CH_3CN using tetrabutyl ammonium perchlorate (TBAP) as supporting electrolyte and platinum as a working electrode. The measurements were carried out in the range 2.2 V to −1.6 V versus SCE (saturated calomel electrode). All the complexes are electroactive, the electrochemical data are presented in Table 3. Representative voltammograms are displayed in Fig. 3.

We first consider the three parent chelates *viz.* **3**, **6** and **8**. Cyclic voltammogram [2] of the reported compound **3** is already discussed. Both **6** and **8** displayed an irreversible oxidation wave at a very high oxidation potential (> 1.6 V) due to $Ru^{II} \rightarrow Ru^{III}$ oxidation. Metal mediated oxidation of coordinated L has recently been discussed in the literature [4]. For the present complexes the oxidation potentials are very high and consequently the chemical reaction succeeding the electrochemical formation of Ru^{III}-L is expected to be very fast and thus the reverse waves were absent in the voltammograms of **6** and **8**. Both the complexes also display reversible, multiple electron transfer reductive responses on the negative of SCE. These are attributed to the reductions of the coordinated ligands. It may be noted that on moving from **3** to **8** *via* **6**, the metal oxidation potential increases in a parallel direction whereas a reverse trend was observed for the ligand reduction. The above trend is as expected, since L^3 stabilizes Ru^{II} better than L due to enhance $d\pi$–$p\pi$ back bonding and also undergoes reduction more easily due to the presence of lower acceptor orbital.

The two monopicolinates **4** and **5** showed reversible oxidative and reductive responses on both positive and negative of SCE. Their metal centered redox potentials are systematically lower than those for the parent diimine compounds. The picolinate ion which is a hard ligand, stabilizes [11] the higher valent state and thus the above shift of redox potential is observed. Moreover, on moving from **4** to **5** the $E_{1/2}$ of Ru^{III}/Ru^{II} couple shifts by about 0.56 V, presumably due to the better stabilisation of lower valent state by L^3 as noted before. For a similar reason, the ligand reductions in

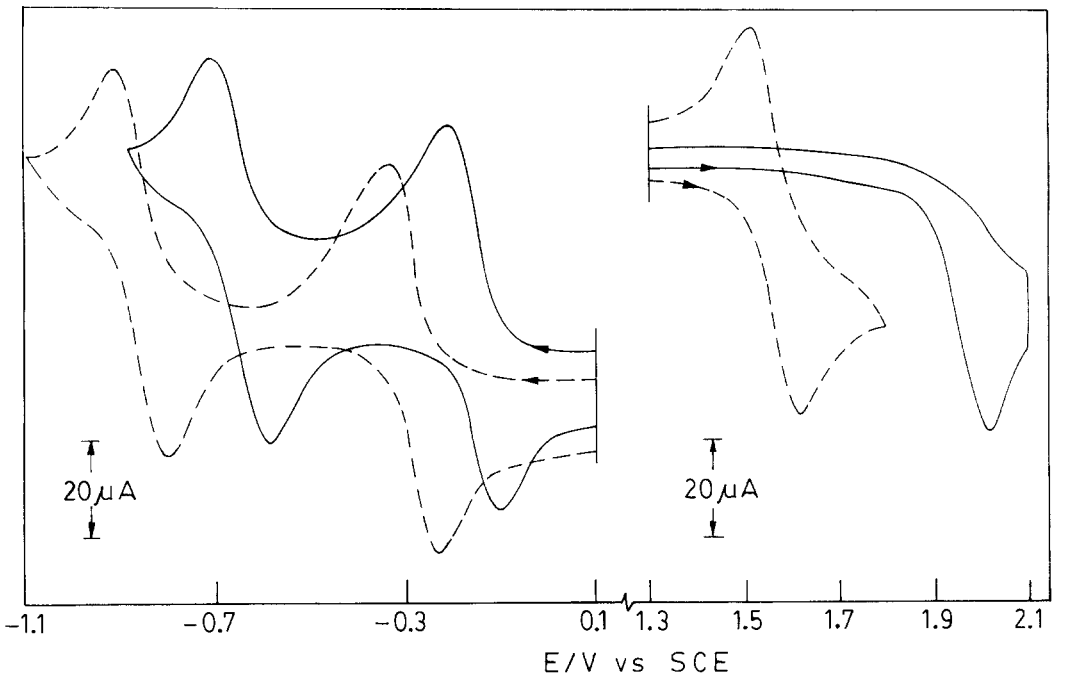

Fig. 3. Cyclic voltammograms of $[Ru(L^2)(L^3)_2](ClO_4)_2 \cdot H_2O$ (——) and $[Ru(pic)(L^3)_2]ClO_4 \cdot CH_2Cl_2$ ( ) in acetonitrile.

5 is easier than that in **4**. The cyclic voltammogram of the monopicolinamide **7** consists of a reversible oxidative response at 1.0 V attributed to Ru^{III}/Ru^{II} couple and two more reductive couples on the negative of SCE due to the ligand reductions.

Interestingly, the metal redox of **4, 5** and **6** are all reversible whereas those of their parents, **3, 6** and **8,** are either irreversible or quasireversible. Irreversibility in the latter group of complexes is due to metal assisted L oxidation reaction. In spite of the fact that both **4** and **6** contain L as coligand their metal redox responses are reversible. It may, therefore, be concluded that partially transformed products, even if they contain additional L, are resistant to further oxidation of L at least in the CV time scale.

The solution absorption spectra of the complexes were recorded in CH_2Cl_2. Representative spectra of the complexes are displayed in Fig. 4 and the data are collected in Tables 4 and 5. Although the complexes retain fairly intense intraligand transitions in the UV region, the key feature is the intense lower energy transitions occurring in the visible region (520–480 nm) those are assigned [2] to $Ru(d\pi) \rightarrow$ ligand (π^*) MLCT transitions. These transition energies for the parent complexes **3, 6** and **8** are systematically higher than those for the monopicolinates **4, 5** and monopicolinamide, **7**. The MLCT absorption energies for all the above complexes, (**3–8**), interestingly, show a linear correlation [2] with ΔE [where, $\Delta E = E_{1/2}(Ru^{III}/Ru^{II}) - E_{1/2}$ (ligand 0/−1)] (Table 5). This correlation, in other words, justifies our assignment of MLCT transitions for the complexes.

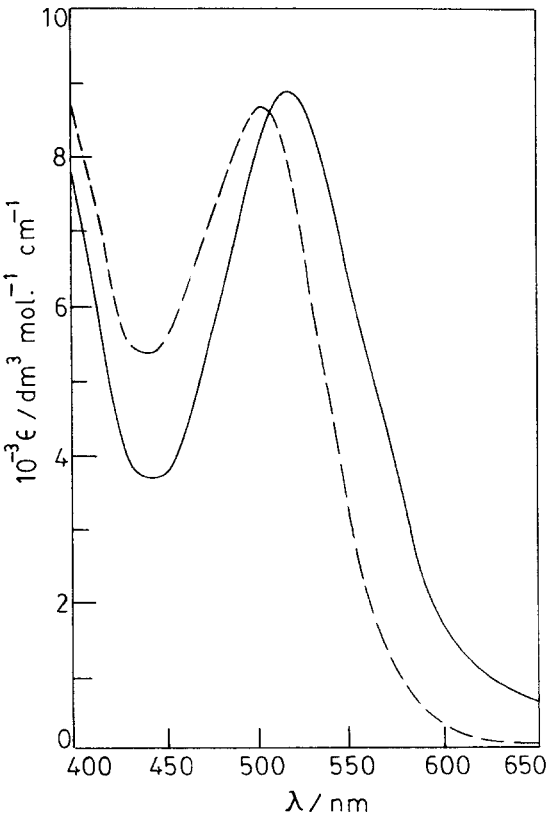

Fig. 4. Visible range absorption spectra of $[Ru(L^2)(L^3)(L^4)]ClO_4 \cdot CH_2Cl_2$ (——) and $[Ru(L^3)(L^2)_2](ClO_4)_2 \cdot H_2O$ (– – –) in CH_2Cl_2.

Table 4. UV–vis spectral data

Compound	Absorption[a] λ_{max} (nm)[δ(mol^{-1}cm^{-1})]
$[Ru(L^1)_3](ClO_4)_2 \cdot H_2O$	480(13760), 445[b](10 880), 300(25 600), 270(25 040)
$[Ru(pic)(L^1)_2]ClO_4 \cdot CH_2Cl_2$	515(10 950), 470[b](7300), 315(23 400), 270(19 040)
$[Ru(L^2)_3](ClO_4)_2 \cdot H_2O$	480(14 310), 445[b](11 120), 315(27 380), 270(25 120)
$[Ru(pic)(L^2)_2]ClO_4 \cdot CH_2Cl_2$	515(11 100), 470[b](7180), 310(23 660), 265(19 175)
$[Ru(L^3)(L^3)_2](ClO_4)_2 \cdot H_2O$	515(7400), 490[c], 370(17270), 320(15 790), 270(15 800)
$[Ru(pic)(L^3)_2]ClO_4 \cdot CH_2Cl_2$	545(11 980), 360(18 620), 310(21 250), 250[b](18 200)
$[Ru(L^3)(L^2)_2](ClO_4)_2 \cdot H_2O$	500(8700), 320(22 960), 265(23 540)
$[Ru(L)(L^3)(L^4)]ClO_4 \cdot CH_2Cl_2$	520(8850), 360[c], 315(23 720)

[a]In MeCN.
[b]Shoulder.
[c]Ill defined shoulder

Finally we wish to mention here that preliminary luminescence studies on the above complexes reveal that the picolinates and the amides have much stronger emission than their parent diimines in the visible region. Our work in this area is continuing.

EXPERIMENTAL

Materials

The salt, $RuCl_3 \cdot nH_2O$ was obtained from Arora Matthey, Calcutta and was digested thrice with concentrated HCl before use. The silver complexes, $[Ag(L)_2]ClO_4$ (L = L^1 or L^2) and $[Ag(L^3)_2]ClO_4$ were synthesized as before [10, 15]. The complexes *cis*-$[RuCl_2(L)_2]$ and *cis*-$[RuCl_2(L^3)_2]$ were prepared [3] by published procedures. The purification of dry solvents for electrochemical and spectral work was performed as described earlier. All other chemicals and solvents used for the preparative work were of reagent grade and were used as received.

Physical measurements

Spectra were recorded on the following equipment: UV–vis, Hitachi 330 spectrophotometer; NMR spectra, Varian XL 200 MHz FT NMR spectrometer. Electrochemical measurements were performed under nitrogen atomosphere on a PAR 370-4 electrochemistry system as described previously [14]. All potentials reported in this work are uncorrected for junction contribution. Solution (*ca* 1 mmol) electrical conductivity measurements were performed on an Elico CM 82T conductivity bridge.

Reactions

(a) Reaction of *cis*-$RuCl_2(L)_2$ (L = L^1 and L^2) and $[Ag(L)_2]ClO_4$. To a sample of bluish green *cis* isomer of $RuCl_2(L)_2$ (0.5 mmol) suspended in ethanol–water mixture (5 : 1) was added a solution of $[Ag(L)_2]ClO_4$ (1 mmol) in ethanol (10 cm^3) and the mixture was heated to reflux for 1 h. The solution was cooled and filtered through a G-4 sintered glass funnel. The filtrate was evaporated to dryness. The crude mass was then dissolved in CH_2Cl_2 and subjected to column chromatography on a silica gel column eluting with different mixtures of CH_2Cl_2-CH_3CN. A pink band of $[Ru(pic)(L)_2]^+$ was eluted with CH_2Cl_2-CH_3CN (5 : 1) followed by a brown band of $[Ru(L)_3]^{2+}$ eluted with CH_2Cl_2-CH_3CN (3 : 2). These were evaporated and crystallized from CH_2Cl_2-C_6H_{14} (1 : 1). The compounds were obtained as solvates. The yields and analyzes were as follows.

Table 5. Redox spectral data

Compound	$E_{1/2}$(V) Metal oxidation	$-E_{1/2}$(V) First ligand reduction	ΔE(V) Ox/Red	*vc.t.* (cm^{-1})
$[Ru(L^1)_3](ClO_4)_2 \cdot H_2O$	1.43	0.93	2.36	20833
$[Ru(pic)(L^1)_2]ClO_4 \cdot CH_2Cl_2$	1.00	1.15	2.15	19417
$[Ru(L^2)_3](ClO_4)_2 \cdot H_2O$	1.44	0.90	2.34	20833
$[Ru(pic)(L^2)_2]ClO_4 \cdot CH_2Cl_2$	1.00	1.16	2.16	19417
$[Ru(L^2)(L^3)_2](ClO_4)_2 \cdot H_2O$	2.00	0.15	2.15	19417
$[Ru(pic)(L^3)_2]ClO_4 \cdot CH_2Cl_2$	1.50	0.28	1.84	18348
$[Ru(L^3)(L^2)_2](ClO_4)_2 \cdot H_2O$	1.81	0.40	2.21	20000
$[Ru(L^2)(L^3)(L^4)]ClO_4 \cdot CH_2Cl_2$	0.98	0.92	1.90	19230

$[Ru(pic)(L^1)_2]ClO_4 \cdot CH_2Cl_2$: yield 35%. (Found: C, 48.3; H, 3.4; N, 9.1. Calc. for $C_{31}N_5H_{26}O_6Cl_3Ru$: C, 48.2; H, 3.4; N, 9.1%).

$[Ru(L^1)_3](ClO_4)_2 \cdot H_2O$: yield 25%. (Found: C, 50.2; H, 3.7; N, 9.6. Calc. for $C_{36}N_6H_{32}O_9Cl_2Ru$: C, 50.0; H, 3.7; N, 9.7%).

$[Ru(pic)(L^2)_2]ClO_4 \cdot CH_2Cl_2$: yield 37%. (Found: C, 49.3; H, 3.7; N, 8.9. Calc. for $C_{33}N_5H_{30}O_6Cl_3Ru$: C, 49.5; H, 3.7; N, 8.7%).

$[Ru(L^2)_3](ClO_4)_2 \cdot H_2O$: yield 26%. (Found: C, 51.5; H, 4.2; N, 9.3. Calc. for $C_{39}N_6H_{38}O_9Cl_2Ru$: C, 51.6; H, 4.2; N, 9.3%).

(b) Conversion of $[Ru(L^1)_3](ClO_4)_2$ to $[Ru(pic)(L^1)_2]ClO_4$. To a solution of 0.25 mmol of $[Ru(L^1)_3](ClO_4)_2$ in ethanol–water mixture (5:1) was added an aqueous solution of $AgNO_3$ (1 mmol in 5 cm^3 of water) and the mixture was heated to reflux for 2 h. It was then evaporated to dryness and subjected to column chromatography on a silica gel column eluting with different mixtures of CH_2Cl_2-CH_3CN as described in Section (a).

The yields were as follows: $[Ru(pic)(L^1)_2]ClO_4 \cdot CH_2Cl_2$: 76%; $[Ru(L^1)_3](ClO_4)_2 \cdot H_2O$: 19%.

(c) Reaction of *cis*-$RuCl_2(L^3)_2$ and $[Ag(L^2)_2]ClO_4$. This reaction was similarly performed as the reaction described in Section (a) starting from *cis*-$RuCl_2(L^3)_2$ and $[Ag(L^2)_2]ClO_4$. The yields and analyzes of the isolated products are as follows:

$[Ru(pic)(L^3)_2]ClO_4 \cdot CH_2Cl_2$: yield 42%. (Found: C, 46.3; H, 3.5; N, 12.2. Calc. for $C_{31}N_7H_{28}O_6Cl_3Ru$: C, 46.4; H, 3.5; N, 12.2%).

$[Ru(L^2)(L^3)_2](ClO_4)_2 \cdot H_2O$: yield 20%. (Found: C, 49.0; H, 3.9; N, 12.4. Calc. for $C_{37}N_8H_{36}O_9Cl_2Ru$: C, 48.9; H, 4.0; N, 12.3%).

(d) Conversion of $[Ru(L^2)(L^3)_2](ClO_4)_2$ to $[Ru(pic)(L^3)_2]ClO_4$. This was similarly performed as described in Section (c) starting from $[Ru(L^2)(L^3)_2](ClO_4)_2$. The yields were as follows: $[Ru(pic)(L^3)_2]ClO_4 \cdot CH_2Cl_2$: yield 85%; $[Ru(L^2)(L^3)_2](ClO_4)_2 \cdot H_2O$: yield 9%.

(e) Reaction of $[Ru(L^3)_2(OH_2)_2]^{2+}$ and PicH was performed as described previously [11].

(f) Reaction of *cis*-$RuCl_2(L^2)_2$ and $[Ag(L^3)_2]ClO_4$. The above reaction was also similarly performed as described in Section (a) starting from *cis*-$RuCl_2(L^2)_2$ and $[Ag(L^3)_2]ClO_4$. The yields and analyzes were as follows:

$[Ru(L^2)(L^3)(L^4)](ClO_4) \cdot CH_2Cl_2$: yield 40%. (Found: C, 52.3; H, 4.0; N, 11.3. Calc. for $C_{39}N_7H_{36}O_5Cl_3Ru$: C, 52.6; H, 4.0; N, 11.0%).

$[Ru(L^3)(L^2)_2](ClO_4)_2 \cdot H_2O$: yield 17%. (Found: C, 50.5; H, 4.1; N, 10.9. Calc. for $C_{38}N_7H_{37}O_9Cl_2$: C, 50.3; H, 4.1; N, 10.8%).

Crystallography

Single crystals of $[Ru(pic)(L^1)_2]ClO_4 \cdot CH_2Cl_2$ were grown at 298 K by slow diffusion of hexane into dichloromethane solution of the compound. Diffraction measurements were carried out on a Nonius CAD4 fully automated four-circle diffractometer. The unit cell was determined and refined using setting angles of 25 reflections, with 2θ angles in the range 11.60 to 20.82°. The unit cell dimensions are listed in Table 6. Data were collected by $\theta - 2\theta$ scans within the angular range 3–45°. All data reduction and structure refinement were performed using the NRCC-SDP-VAX packages. The structure was solved by the Patterson method. Final cycles of least square refinement converged with discrepancy indices of $R_f = 0.045$ and $Rw = 0.035$. Tables containing full listings of atom positions, anisotropic thermal parameters and hydrogen atom locations are available as supplementary material.

Table 6. Crystallographic data for $[Ru(pic)(L^1)_2]ClO_4 \cdot CH_2Cl_2$

Formula	$RuC_{31}H_{26}N_5Cl_3O_6$
fw	772.00
Crystal system	Triclinic
Space group	*P*-1
a (Å)	11.3737(23)
b (Å)	12.527(3)
c (Å)	13.255(3)
α (°)	71.978(20)
β (°)	66.052(19)
γ (°)	75.476(18)
V (Å^3)	1624.1
Z	2
D_{calc} (gm cm^{-3})	1.579
μ (cm^{-1})	7.028
Crystal size (mm)	$0.05 \times 0.05 \times 0.30$
λ (Å)	0.7107
T (K)	298
R_f, *Rw*	0.045, 0.035
GOF	1.61

Acknowledgement—Financial support received from the University Grants Commission, New Delhi is gratefully acknowledged.

REFERENCES

1. See, for Example, E. A. Seddon and K. R. Seddon, *The Chemistry of Ruthenium*, pp 414, 1173. Elsevier, New York (1984); G. Wilkinson, R. D. Gillard and J. A. McCleverty, *Comprehensive Coordination Chemistry*, vol. 4, p. 277. Pergamon, Oxford (1987); T. J. Meyer, *Pure Appl. Chem.* 1986, **58,** 1193; A. Juris, V. Balzani, F. Barigelletti, S. Campagna, P. Belser and A. von. Zelewsky, *Coord. Chem. Rev.* 1988, **84,** 85; H. Masui, A. B. P. Lever and E. S. Dodsworth, *Inorg. Chem.* 1993, **22,** 258; R. M. Berger and J. R. Holcombe, *Inorg. Chim. Acta* 1995, **232,** 217; F. Hartl, T. L. Snoeck, D. J. Stufkens and A. B. P. Lever, *Inorg. Chem.* 1995, **34,** 3887; M. Maruyama, H. Matsuzawa and Y. Kaizu, *Inorg. Chem.* 1995, **34,** 3232.

2. S. Choudhury, A. K. Deb and S. Goswami, *J. Chem. Soc., Dalton Trans.* 1994, 1305.
3. S. Choudhury, M. Kakoti, A. K. Deb and S. Goswami, *Polyhedron* 1992, **11,** 3183.
4. M. Menon, S. Choudhury, A. Pramanik, A. K. Deb, S. K. Chandra, N. Bag, S. Goswami and A. Chakravorty, *J. Chem. Soc., Chem. Commun.* 1994, 57.
5. E. V. Dose and L. J. Wilson, *Inorg. Chem.* 1978, **17,** 2600.
6. P. Belser and A. von Zelewsky, *Helv. Chim. Acta* 1980, **63,** 1675.
7. M. Kakoti, A. K. Deb and S. Goswami, *Inorg. Chem.* 1992, **31,** 1302.
8. A. K. Deb, M. Kakoti and S. Goswami, *J. Chem. Soc., Dalton Trans.* 1991, 3249.
9. S. Choudhury, A. K. Deb, W. Kharmawphlang and S. Goswami, *Proc. Indian Acad. Sci. (Chem. Sci.).* 1994, **106,** 665.
10. S. Choudhury, A. K. Deb and S. Goswami, *Polyhedron* 1994, **13,** 1063.
11. N. Chatak and S. Bhattacharya, *Polyhedron* 1994, **13,** 2999; N. Ghatak, J. Chakravarty and S. Bhattacharya, *Trans. Met. Chem.* 1995, **20,** 138.
12. M. C. Barral, R. J. Aparicio, E. C. Royer, M. J. Saucedo, F. A. Urbanos, E. G. Puebla, C. R. Valero, *J. Chem. Soc., Dalton Trans.* 1991, 1609.
13. M. Menon, A. Pramanik and A. Chakravorty, *Inorg. Chem.* 1995, **34,** 3310.
14. S. Goswami, R. N. Mukherjee and A. Chakravorty, *Inorg. Chem.* 1983, **22,** 2825.
15. A. K. Deb, S. Choudhury and S. Goswami, *Polyhedron* 1990, **9,** 2251.
16. G. F. Strouse, P. A. Anderson, J. R. Schoonover, T. J. Meyer and F. R. Keene, *Inorg. Chem.* 1995, **31,** 3004.
17. R. H. Keyser and R. M. Pollack, *J. Am. Chem. Soc.* 1977, **99,** 3379.